



Consistent formulation of the crossover from density to velocity dependent recombination in organic solar cells

Mehdi Ansari-Rad,^{1,a)} Germà Garcia-Belmonte,² and Juan Bisquert^{2,3}

¹Department of Physics, University of Shahrood, Shahrood, Iran

²Institute of Advanced Materials (INAM), Universitat Jaume I, 12006 Castelló, Spain

³Department of Chemistry, Faculty of Science, King Abdulaziz University, Jeddah, Saudi Arabia

(Received 3 May 2015; accepted 7 August 2015; published online 17 August 2015)

Carrier recombination is a central process in bulk heterojunction organic solar cells. Based on the competition of hopping rates that either implies escape in a broad density of states or recombination across the interface, we formulate a general theory of recombination flux that distinguishes reaction or transport limited recombination according to charge density. The Langevin picture is valid only in the low charge density limit, and a crossover to the reaction controlled regime occurs at higher densities. We present results from impedance spectroscopy of poly(3-hexylthiophene):methanofullerene solar cell that exhibit this crossover. © 2015 AIP Publishing LLC. [<http://dx.doi.org/10.1063/1.4928758>]

Organic bulk heterojunction (BHJ) solar cells comprise a blend of a conjugated polymer (donor) and a fullerene (acceptor), interpenetrated on the nanometer scale.¹ One of the main loss mechanism limiting the open-circuit photovoltage of BHJ solar cells is nongeminate recombination of electrons and holes at the donor-acceptor interface.² For this reason, a profound understanding of the underlying physics behind the recombination process is of great importance³ both for improving the solar cell efficiency and for developing alternative optoelectronic applications of the organic blends such as organic light emitting diodes and photodetectors.

Recombination rates applied to describe the nongeminate recombination in BHJs can be expressed in a general bimolecular form as $R = Cnp$, where n and p are the electron and hole density, respectively. The recombination coefficient C contains the physics of the recombination process and it has been investigated by a combination of experimental techniques⁴ as time-resolved charge extraction (TRCE), transient absorption spectroscopy (TAS), photoinduced charge extraction by linearly increasing voltage (photo-CELIV), transient photovoltage, and impedance spectroscopy,^{5,6} but a general picture on its physical interpretation has not yet been established.⁷ If C is completely independent of the mobility of the carriers, one deals with a reaction-limited recombination. Such a mechanism has first been utilized to describe the recombination in dye-sensitized solar cells, and then extended to the case of the BHJs.⁸ However, the widespread assumption is that the nongeminate recombination in BHJs is a diffusion-limited process:⁹ electron and hole most likely recombine, nonradiatively, upon their first encounter at the donor-acceptor interface. According to the classical Langevin theory, the prefactor C is then directly proportional to effective mobility by which electron and hole find each other. It has been generally observed that the description of carrier lifetimes in BHJ requires to consider a broad distribution of localized states.^{10–12} Recently, trap-assisted recombination model

based on the Shockley-Read-Hall (SRH) recombination picture has been developed in the field of BHJs.^{13,14} For free carriers with mobilities μ_n^f and μ_p^f , together with the assumption of the diffusion-limited nature of recombination, this approach leads to a recombination rate as¹³

$$R \sim \mu_n^f n_f p. \quad (1)$$

There is, however, no *a priori* reason that recombination in BHJs should be diffusion controlled. Despite the experimental evidence in favor of this model, there are also experimental results that give a different density dependence for the prefactor C than that measured for the mobility.^{15–17} In addition, SRH model assumes two classes of carriers in the system, free and trapped carriers, which are different in nature from each other. But, in disordered systems as BHJ blends, one cannot establish a distinction between free and trapped carriers. The disparity of experimental findings suggests that a more complex recombination mechanism occurs in BHJ blends, which may be eventually reduced to either density or diffusion controlled phenomenological regimes, according to microscopic parameters that describe the rich morphology, energetic landscape, and particularities of the organic blends.

Our approach consists on a formulation of fundamental hopping rates of localized electron and holes. In this approach, all charge carriers move between the localized sites, more rapidly or slowly, depending on the energy of the localized state they reside in. In order to determine the probability of escape of one carrier from a recombination site at the donor-acceptor interface, we use the standard transport energy concept, which is a unique energy level, E_{tr} , that determines the fastest upward hopping events.¹⁸ This model can reproduce both the diffusion- and reaction-limited regime, depending on the carrier density in the system, and furthermore quantitative criteria are established that determine the dominant recombination regime. A comparison with experimental results really explains a crossover between two regimes for the recombination resistance of a poly(3-hexylthiophene):[6,6]-phenyl C61-butyric acid methyl ester (P3HT:PCBM) BHJ solar cell.

^{a)}Electronic mail: ansari.rad@shahroodut.ac.ir

We study transfer of electrons from a distribution of localized trap states $g(E)$ to that of holes. Carriers move via the hopping mechanism between the localized states. The hopping rate ν_{ij} from energy E_i to an empty state E_j is given by the Miller-Abrahams expression.¹⁹ We are interested in recombination at steady-state open-circuit conditions in which electrons and holes have relaxed to well-defined, spatially homogeneous, Fermi-levels E_{fn} and E_{fp} , respectively,²⁰ so that occupancy of the density of states (DOS) is given by the Fermi function $f(E, E_{fn}) = \{1 + \exp[(E - E_{fn})/k_B T]\}^{-1}$, where $k_B T$ is the thermal energy. Voltage of the cell is related to the separation of the Fermi-levels as $qV = E_{fn} - E_{fp}$, where q is elementary charge.

Let us focus on the dynamics of an electron in the acceptor phase. As depicted in Fig. 1(a), at the interface region, we must consider competition of the recombination with the transport: the electron either jump to the neighbouring traps with the rate $\sum_j \nu_{ij}$ or recombine with a hole, with a frequency K . The hole is considered to be immobile during a recombination event. This means that $\mu_n > \mu_p$, which is generally true in BHJ devices,²¹ where μ_n and μ_p are the total electron and hole mobility, respectively. At the interface, the frequency K is, in fact, in competition with the fastest hop expressed as $\nu(E) = \bar{\nu}_0 \exp[(E - E_{tr})/k_B T]$. $\bar{\nu}_0$, the effective attempt-to-jump frequency, will be of great importance to this model since it gives the time constant of the transport. It also gives the average downward hopping rate, from the transport energy E_{tr} into the nearest trap. For the Gaussian DOS, most relevant to organic blends, E_{tr} lies around the center of the Gaussian, the acceptor lowest-unoccupied molecular orbital (LUMO).^{22,23} Average probability of the recombination at each step of the hopping can then be expressed as

$$\Gamma = \gamma \left\langle \frac{K}{\nu(E) + K} \right\rangle. \quad (2)$$

The dimensionless parameter $\gamma = \kappa p$ accounts for the fact that there will be a probability for the recombination only when there is both an electron near the interface and a hole near the interface too. κ , the effective space available for the recombination, is related to the spatial extension of the electron and hole wavefunctions.

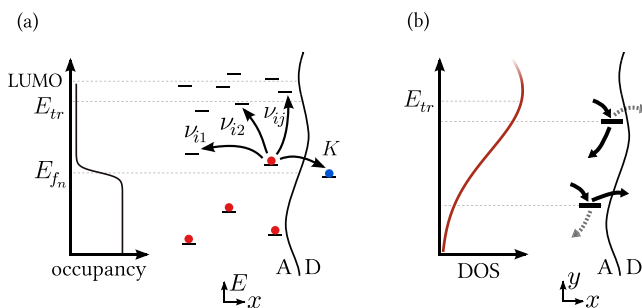


FIG. 1. (a) Scheme of the model used to describe the charge recombination in BHJs (A: acceptor, D: donor). The most probable jump (ν) of the electron is to a neighbouring trap with energy E_{tr} which lies well above the Fermi-level E_{fn} . K is the recombination frequency. (b) Illustration showing how the energy of the trap involved in the recombination process determines the recombination nature. The carrier most likely recombines (escapes from the interface) when becoming localized into a deep (shallow) trap.

Total recombination rate can be calculated using the definition $R = n/\tau$, where τ is the lifetime of the electron given as $\tau = \langle t \rangle / \Gamma$.^{24,25} Here, $\langle t \rangle$ is the average time that electron spends in a trap. Using the method used in Ref. 23 to calculate these average quantities and by straightforward algebraic manipulation, we finally get a general expression for the recombination rate as follows:

$$R = \kappa p \int_{-\infty}^{E_{tr}} \frac{\nu(E) K}{\nu(E) + K} g(E) f(E, E_{fn}) dE. \quad (3)$$

As seen in Eq. (3), both the recombination frequency K and the transport frequency ν are determining factors in the total recombination flux. It must be noted that a similar approach was used in Ref. 25 to obtain an expression for the recombination rate. But competition between the transport and recombination process was not considered in the formulation, leading to a reaction-limited recombination rate. In contrast, as we discuss, Eq. (3) provides a general rate that encompasses the different dynamic regimes. In the following, we provide a physical insight into the recombination mechanism suggested by Eq. (3).

For sufficiently deep energy levels (with respect to the transport energy) $K \gg \nu(E)$. Physically, this means that when the electron reaches the interface and gets localized in a deep state, it will have a small chance to escape, and most probably finally recombines, after a time $t \sim 1/K$; see Fig. 1(b). This behavior is clearly a signature of the diffusion-limited recombination. At low voltage, nearly all electrons are localized in the deep levels, and we can consider the condition $K \gg \nu(E)$ to hold for most electrons. In this case, using the relation $\mu_n/n \propto \int \nu(E) g(E) f(E, E_{fn}) dE$,²⁶ our general expression for R is simplified as

$$R \propto \mu_n n p, \quad (4)$$

which is a Langevin-like recombination rate. Note that Eq. (1) can also be written in the form of the above equation, using the fact that based on the trap-assisted transport model $n\mu_n = n_f \mu_n^f$.²⁷ Despite this mathematically similar form for the recombination rates, however, in contrast to the assumptions behind Eq. (1), in our approach all carriers contribute to the recombination, not just those, say, in the vicinity of the transport energy.

We now discuss the opposite case of shallow energy levels in which $K \ll \nu(E)$. Because of the very short residence time of the carrier localized in a shallow trap, the chance of being captured by a hole is small and the carrier will escape from the interface, as shown schematically in Fig. 1(b). At high charge densities, most carriers are localized in these shallow states. In this case, the general recombination rate of Eq. (3) is simplified as

$$R = K' n p, \quad (5)$$

with $K' = \kappa K$. This rate is independent of the transport speed, because $\bar{\nu}_0$ is absent in the expression. Therefore, recombination mechanism in this situation is reaction-limited. Note that to provide more physical insight into the recombination mechanism, the recombination frequency K

was considered independent of the energy of the carriers, in agreement with experimental results.²⁸ This is similar to the assumption made in the SRH approach that capture cross sections are independent of the energy.²⁹ This simplification can easily be relaxed, for example, by using a Marcus-type charge transfer rate for the recombination frequency.^{8,11}

Eqs. (4) and (5) show that the general expression obtained here for the recombination rate can naturally produce both the Langevin(-like) and the reaction-limited recombination rate. We remark however that the two regimes simultaneously contribute to recombination flux at large charge densities. The change of the recombination from the diffusion- to reaction-limited rate does occur when the density is increased, simply due to the fact that deep traps will be inaccessible for most carriers.

An ideal quantity to study the recombination rate is the recombination resistance, which can be directly observed in impedance spectroscopy measurement, and is related to the recombination rate as

$$r_{\text{rec}} = \frac{1}{qL} \left(\frac{dR}{dV} \right)^{-1}, \quad (6)$$

with L being the active layer thickness. Therefore, to provide experimental evidence for the crossover, we present and discuss results from the impedance spectroscopy of a typical P3HT:PCBM BHJ solar cell, with efficiency of 3% at 1 sun.³⁰ Fig. 2 shows the recombination resistance extracted from the impedance spectroscopy as a function of the voltage V . Each data point in the figure corresponds to a specific light intensity and applied voltage. Because of a voltage drop due to series resistance, applied voltage to the cell differs from the voltage V that is given by the Fermi-levels separation. Fortunately, this resistance can also be extracted from the impedance measurement and the result can then be used to correct the voltage

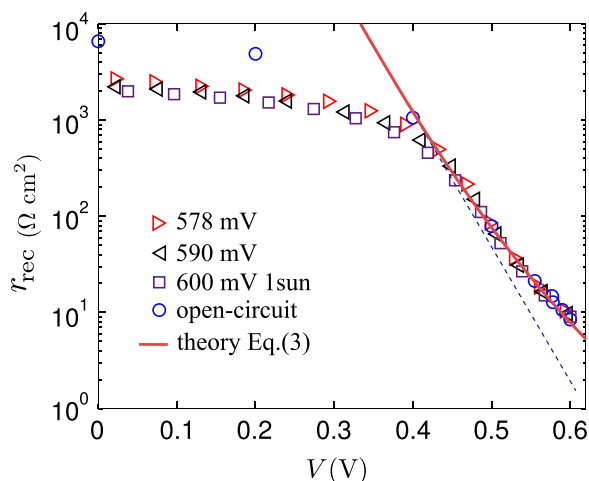


FIG. 2. Recombination resistance vs. voltage obtained at room temperature from impedance spectroscopy, measured using two different conditions: (1) at three different illumination intensities (corresponding to the open-circuit voltage shown) and applied bias and (2) at open-circuit conditions (varying the illumination intensity). Voltage corresponds to the internal Fermi level splitting that results after removing the series resistance potential drop. Solid line shows fit to Eq. (3) with $N = 0.007 \text{ nm}^{-3}$, $\sigma = 0.11 \text{ eV}$, $\text{LUMO-HOMO} = 1.1 \text{ eV}$, $\kappa = 0.28 \text{ nm}^3$, $K = 10^{-3} \text{ THz}$, and $\bar{v}_0 = 10^2 \text{ THz}$. Dashed line shows the curve with the slope resulted from the pure diffusion-limited rate.

scale,³¹ as done for the result in Fig. 2, so that voltage V directly represents separation of Fermi-levels (at low voltage r_{rec} is still contaminated by the effect of the shunt resistance). Fit of the recombination resistance data by Eq. (3) is also shown in the figure. Gaussian DOS was used in the fitting, in form of $g(E) = N/\sqrt{2\pi\sigma^2} \exp[-(E - \text{LUMO})^2/2\sigma^2]$ for the electrons, and one centered at donor highest-occupied molecular orbital (HOMO) for the holes. Here, N is the total density of localized states and σ is the width. E_{rr} was considered to be pinned at LUMO, which is true in the range of the carrier density studied here ($n/N \leq 0.02$).²² As seen in Fig. 2, the theory can reproduce the experiment well, in the region that the shunt resistance does not affect r_{rec} . For comparison, the curve with the slope given by a pure diffusion-limited mechanism is also depicted in the figure. The curve deviates from the experimental data at high voltage that, based on our model, is because of change in the recombination mechanism at high carrier density.

Let us finally briefly discuss how the picture of recombination provided here can interpret experimental trends concerning the bimolecular recombination coefficient, the prefactor C in $R = Cnp$, in BHJs. (i) Change in the recombination mechanism implies that the recombination coefficient is not necessarily given by the mobility. Therefore, a different density dependence, than that measured for the mobility, may be obtained for the coefficient C , as indeed observed in BHJs.^{15,16} (ii) Diffusion-to-reaction limited crossover occurs smoothly, so that at the intermediate carrier density the system is, in fact, in a mixed regime of the recombination. Carriers localized in the shallow energy levels have the most contribution to the total mobility, but recombine as reaction-limited. In the other words, their contribution to the mobility does not enter into the diffusion-limited part of the recombination rate. This can explain the so-called reduced bimolecular recombination rate, upon which the prefactor C is usually observed to be one to three orders of magnitude lower than one predicted by the Langevin recombination mechanism. Using the parameters obtained from the fitting in Fig. 2, we calculate the prefactor C as a function of the density. Fig. 3 shows the result. Result of the calculation using the same parameters but with $K \rightarrow \infty$ (diffusion-limited conditions) is also presented. As seen, a reduction factor of $< 10^{-2}$ is obtained from the comparison. This justifies that the origin of the reduced bimolecular recombination rate can be deviation of the recombination mechanism from a purely Langevin-like recombination process. Carrier density gradient across the cell has also been proposed to be responsible for the effect.^{32,33}

In conclusion, we have presented a unified description for the nongeminate recombination in the energy disordered blends that produces naturally both the diffusion- and reaction-limited regime. Our formulation predicts a crossover between these two regimes by change in the carrier density, as a consequence of the increasing role of shallow localized states in the recombination process. We discussed how this can explain experimental results obtained for a typical P3HT:PCBM solar cell. The picture provided here gives insights into the mechanism of the electron-hole recombination in the energy-disordered materials. This knowledge helps finding ways to improve the solar cell efficiency, as it

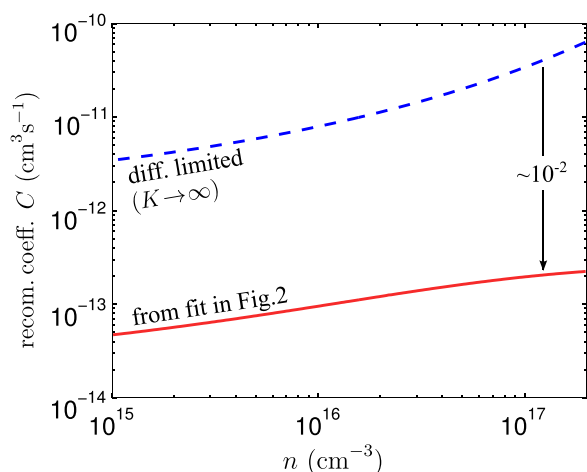


FIG. 3. Bimolecular recombination coefficient C vs. charge density n . Solid line shows Eq. (3) using the parameters obtained from fitting in Fig. 2, see the figure caption. Dashed line is calculated using the same parameter but with the recombination frequency $K \rightarrow \infty$. The range of the density n corresponds to the voltage $0.4 \leq V \leq 0.6$.

provides insight for the interpretation of the measurements in BHJs. Our finding suggests that the recombination mechanism at the normal operating conditions of the solar cell is, in practice, reaction limited. We therefore think in order to improve the open-circuit photovoltage of P3HT:PCBM solar cells, the efforts should be focused on the specific chemical features of the charge-transfer process at the interface between the acceptor molecules and the donor polymer, and not on the carrier mobility.

The work was supported by Generalitat Valenciana (Project No. ISIC/2012/008). We are grateful to J. A. Anta for useful discussions.

¹C. Deibel and V. Dyakonov, *Rep. Prog. Phys.* **73**, 096401 (2010).

²S. R. Cowan, N. Banerji, W. L. Leong, and A. J. Heeger, *Adv. Funct. Mater.* **22**, 1116 (2012).

³D. Bozyigit, W. M. Lin, N. Yazdani, O. Yarema, and V. Wood, *Nat. Commun.* **6**, 6180 (2015).

⁴T. M. Clarke, C. Lungenschmied, J. Peet, N. Drolet, and A. J. Mozer, *Adv. Energy Mater.* **5**, 1401345 (2015).

⁵L. Xu, Y.-J. Lee, and J. W. Hsu, *Appl. Phys. Lett.* **105**, 123904 (2014).

⁶B. J. Leever, C. A. Bailey, T. J. Marks, M. C. Hersam, and M. F. Durstock, *Adv. Energy Mater.* **2**, 120 (2012).

⁷T. Kirchartz and J. Nelson, *Phys. Rev. B* **86**, 165201 (2012).

⁸G. Garcia-Belmonte, P. P. Boix, J. Bisquert, M. Sessolo, and H. J. Bolink, *Sol. Energy Mater. Sol. Cells* **94**, 366 (2010).

⁹C. M. Proctor, M. Kuik, and T.-Q. Nguyen, *Prog. Polym. Sci.* **38**, 1941 (2013).

¹⁰A. Pivrikas, H. Neugebauer, and N. S. Sariciftci, *IEEE J. Sel. Top. Quantum Electron.* **16**, 1746 (2010).

¹¹G. Garcia-Belmonte and J. Bisquert, *Appl. Phys. Lett.* **96**, 113301 (2010).

¹²A. Fallahpour, A. Gagliardi, F. Santoni, D. Gentilini, A. Zampetti, M. A. der Maur, and A. Di Carlo, *J. Appl. Phys.* **116**, 184502 (2014).

¹³T. Kirchartz, B. E. Pieters, J. Kirkpatrick, U. Rau, and J. Nelson, *Phys. Rev. B* **83**, 115209 (2011).

¹⁴M. Kuik, L. J. A. Koster, G. A. H. Wetzelaer, and P. W. M. Blom, *Phys. Rev. Lett.* **107**, 256805 (2011).

¹⁵D. Rauh, C. Deibel, and V. Dyakonov, *Adv. Funct. Mater.* **22**, 3371 (2012).

¹⁶S. A. Hawks, F. Deledalle, J. Yao, D. G. Rebois, G. Li, J. Nelson, Y. Yang, T. Kirchartz, and J. R. Durrant, *Adv. Energy Mater.* **3**, 1201 (2013).

¹⁷Y. Preezant and N. Tessler, *J. Appl. Phys.* **109**, 013701 (2011).

¹⁸D. Monroe, *Phys. Rev. Lett.* **54**, 146 (1985).

¹⁹S. Baranovskii, *Charge Transport in Disordered Solids with Applications in Electronics* (John Wiley & Sons, 2006).

²⁰J. Bisquert and G. Garcia-Belmonte, *J. Phys. Chem. Lett.* **2**, 1950 (2011).

²¹L. Koster, V. Mihailetchi, and P. Blom, *Appl. Phys. Lett.* **88**, 052104 (2006).

²²J. Oelerich, D. Huemmer, M. Weseloh, and S. Baranovskii, *Appl. Phys. Lett.* **97**, 143302 (2010).

²³J. Oelerich, D. Huemmer, and S. Baranovskii, *Phys. Rev. Lett.* **108**, 226403 (2012).

²⁴M. Ansari-Rad, J. A. Anta, and J. Bisquert, *J. Phys. Chem. C* **117**, 16275 (2013).

²⁵M. Ansari-Rad, J. A. Anta, and E. Arzi, *J. Chem. Phys.* **140**, 134702 (2014).

²⁶V. Arkhipov, P. Heremans, E. Emelianova, G. Adriaenssens, and H. Bässler, *Appl. Phys. Lett.* **82**, 3245 (2003).

²⁷J. Bisquert, *Phys. Chem. Chem. Phys.* **10**, 3175 (2008).

²⁸A. Guerrero, L. F. Marchesi, P. P. Boix, J. Bisquert, and G. Garcia-Belmonte, *J. Phys. Chem. Lett.* **3**, 1386 (2012).

²⁹W. Shockley and W. T. Read, *Phys. Rev.* **87**, 835 (1952).

³⁰See supplementary material at <http://dx.doi.org/10.1063/1.4928758> for details of the solar cell preparation.

³¹P. P. Boix, A. Guerrero, L. F. Marchesi, G. Garcia-Belmonte, and J. Bisquert, *Adv. Energy Mater.* **1**, 1073 (2011).

³²C. Deibel, A. Wagenpfahl, and V. Dyakonov, *Phys. Rev. B* **80**, 075203 (2009).

³³F. Deledalle, P. Shakya Tuladhar, J. Nelson, J. R. Durrant, and T. Kirchartz, *J. Phys. Chem. C* **118**, 8837 (2014).